Adhesion of Thin, Dry Block Copolymer Layers Adsorbed on Mica

Hiroshi Watanabe,*,† Shigetomo Matsuyama,‡ Yoshinori Mizutani,‡,§ and Tadao Kotaka‡

Institute for Chemical Research, Kyoto University, Uji, Kyoto 611, Japan, and Department of Macromolecular Science, Faculty of Science, Osaka University, Toyonaka, Osaka 560, Japan

Received January 3, 1995; Revised Manuscript Received May 30, 1995®

ABSTRACT: Adhesion was examined for dry, thin layers of poly(2-vinylpyridine) (PVP)–polyisoprene (PI) diblock and graft-block copolymers, the latter having PVP blocks as the trunk and PI blocks as the branch. Those copolymers were selectively adsorbed at the PVP blocks on mica from toluene solutions. *In toluene* the diblock and graft-block copolymers appeared to obey the same thermodynamics of adsorption that was discussed by Parsonage et al. *In dry states* the adsorbed copolymers formed *very thin* layers having the PVP blocks at the bottom and the PI blocks at the top, and adhesion of those layers was related to interaction of the PI blocks having entropically unfavorable, flattened conformations. Adhesion energies per unit area (surface free energy decrease on contact), γ, were measured for two cases, *symmetric* or *asymmetric* contact of identical or different PI block layers. For both cases γ was larger than the surface energy per unit area, $\gamma_{\text{homo-PI}}$, for homo-PI films of macroscopic size. $\gamma_{\text{homo-PI}}$ represented the van der Waals contribution to adhesion, and the extra adhesion energy for the PI blocks, γ-$\gamma_{\text{homo-PI}}$, was related to their flattened conformation: On contact of two adsorbed layers, the PI blocks belonging to each layer could interpenetrate each other and increase their conformational entropy. This entropy gain was considered to be the origin of the extra adhesion. For both symmetric and asymmetric contacts, the extra adhesion energy *reduced per PI block*, $\Delta\gamma^*$, was found to be proportional to N^*kT, with N^* and kT being the PI block length normalized by the PI layer thickness and the thermal energy, respectively. This proportionality as well as the $\Delta\gamma^*$ values themselves were satisfactorily explained from a calculation of entropy gain for confined tethered chains brought into contact, supporting the validity of the above mechanism of the extra adhesion. The adhesion energies of the adsorbed copolymer layers were also discussed in relation to a stretched-chain pullout mechanism experimentally observed by Creton et al.

I. Introduction

Adsorption of polymer chains offers an interesting field of polymer physics and also enables a wide variety of applications like surface modification and stabilization of colloidal particles.[1-3] Because of such scientific as well as practical importance, interactions between adsorbed chains have been extensively studied,[1,2] in particular for some model polymers, poly(2-vinylpyridine)–polystyrene (PVP–PS) and PVP–polyisoprene (PVP–PI) diblock copolymers[4-7] and end-functionalized PS chains.[8,9]

The interaction in solvents is rather well understood.[1,4-9] In toluene, a good solvent for PS and PI but a nonsolvent for PVP, the above model polymers are selectively adsorbed on mica at the PVP blocks and/or functionalized ends. The nonadsorbed PS and/or PI blocks having tethered conformations are stretched in the direction normal to the mica surface to form so-called *polymer brushes*[1] (unless the adsorbed amount is very small). Extensive surface force measurements established that two brush layers compressed with each other exhibit monotonically increasing repulsion.[4-9] This repulsive interaction, reflecting the osmotic and elastic free energies of the brush layers,[1,4-9] is successfully described by theories[5,10] that consider a balance of these energies (for compression of two identical layers).

The other type of interesting interaction, adhesive interaction, was also found for the adsorbed PVP–PS and PVP–PI block copolymers in *dry* states.[6] An adhesion energy (surface free energy decrease on contact), γ, was determined by interactions of the PS or PI blocks located at the top of the dry, adsorbed layers. Those layers had thicknesses much smaller than the unperturbed dimension of the blocks. Thus, in contrast to the stretched brush conformation in toluene, the PS and PI blocks took flattened conformations in the dry layers. For a PVP–PS sample with $M_{\text{PVP}} = M_{\text{PS}} = 60$k, γ at 32 °C was comparable to the surface energy for bulk homo-PS films.[6] This result indicates that the van der Waals attraction dominates the adhesion of the thin PS block layers (in the glassy state). On the other hand, γ of a PVP–PI sample ($M_{\text{PVP}} = 30$k and $M_{\text{PI}} = 217$k) was considerably larger than the surface energy of bulk homo-PI films.[6] In a previous study, this enhancement of adhesion for the PI blocks (in the rubbery state) was attributed to their flattened conformation:[6] On contact of two identical adsorbed layers, the PI blocks belonging to each layer gain a space twice as large and thus a larger conformational freedom. Then, they should interpenetrate with each other to increase the conformational entropy. This entropy gain was considered to be the origin of the enhanced adhesion. This type of enhancement does not emerge in the glassy state (where the chain motion is frozen and no interpenetration takes place) and is in harmony with the observation for the PS blocks.

The previous study examined adhesion for one particular PVP–PI copolymer and proposed the above mechanism of the enhancement of adhesion.[6] For further investigation of this mechanism, we have measured the adsorbed amount σ and adhesion energies γ

* To whom correspondence should be addressed.
† Kyoto University (previously at Osaka University).
‡ Osaka University.
§ Current address: Engineering Department, Toyoda Automatic Loom Works, Ltd., Obu, Aichi 474, Japan.
® Abstract published in *Advance ACS Abstracts*, August 15, 1995.

0024-9297/95/2228-6454$09.00/0

Table 1. Characteristics of PVP–PI Diblock Copolymer Samples[a]

code	10^{-3}-M_{PVP}[b]	$(M_w/M_n)^{PVP-PI}$	10^{-3}-M_{PI}[b]	$(M_w/M_n)^{PI}$
PVP–PI 1–18	1.1	1.08	17.6	1.04
PVP–PI 49–32	48.5	1.07	31.9	1.05
PVP–PI 15–73	14.5	1.09	73.0	1.05
PVP–PI 34–73	33.7	1.09	73.0	1.05
PVP–PI 72–73	72.1	1.04	73.0	1.05
PVP–PI 102–164	102	1.10	164	1.05
PVP–PI 72–338	72.1	1.14	338	1.06

[a] PI microstructure: cis/trans/vinyl ≅ 75/20/5.[16] [b] Weight-average molecular weight.

for layers of various PVP–PI diblock and PVP–$(PI)_x$ graft-block (comb) copolymers of different M_{PVP} and M_{PI}. This paper presents the results. In section III-1, our σ data are compared with those reported by Parsonage et al.[11] and the adsorption behavior is discussed. Sections III-2 and III-3, respectively, examine the central issue of this paper, adhesion energies γ for *symmetric* and *asymmetric* contacts of *identical* and *different* copolymer layers. Specifically, the σ and M_{PI} dependence of γ is examined in relation to the previously proposed mechanism.[6] In section III-4, this dependence is compared with the results found in a recent study of Creton, Brown, and Shull[12] for adhesion of PS–PI copolymer layers and *cross-linked* PI networks. A stretched-chain pullout mechanism[13,14] explaining their adhesion data[12] is examined for our adsorbed copolymer layers. Finally, section IV presents a summary of this study.

II. Experimental Section

Materials. PVP–PI diblock copolymers were synthesized *via* sequential anionic polymerization in high vacuum: The PI blocks were polymerized with *sec*-butyllithium in heptane, and the PVP blocks were copolymerized after switching the solvent to THF. PVP–$(PI)_x$ *graft-block* (comb) copolymers having the PVP blocks as the trunks and the PI blocks as the branches were synthesized *via* a grafting reaction of PI prepolymer anions onto homo-PVP (nitranion formation):[15] The PI anions were grafted up to a saturation point, and excess PI prepolymers were removed by fractionation. Details of these synthetic procedures were reported elsewhere.[6,15] A small amount (<0.5%) of an antioxidant (2,6-di-*tert*-butyl-4-methylphenol) was added to the diblock and graft-block copolymer samples.

The copolymers were characterized with GPC (Tosoh HLC-801A) having an ultraviolet (UV) spectrometer (Tosoh UV-8000) and a combined refractive index (RI) and low-angle laser light scattering (LS) detector (Tosoh LS-8000). The elution solvent was THF, and antiadsorption columns (Tosoh G-4000 H_{XL} and G-5000 H_{XL}) were used. Previously synthesized and characterized homo-PI samples[16] were used as the elution standards.

Tables 1 and 2 summarize the characteristics of the diblock and graft-block copolymers. The code numbers indicate the block (or prepolymer) molecular weights in units of 1000. For the PVP–$(PI)_x$ graft-block copolymers (Table 2), the index x represents the number of PI branches per PVP trunk, and M_{span} is the average molecular weight of the PVP span between the neighboring PI branches.[15] Note that some copolymers, synthesized from the same batch of the PI prepolymer anions, have the same PI block length (M_{PI} = 17.6k and/or 73k; cf. Tables 1 and 2).

Adsorbed Layer Preparation. Dry, adsorbed layers of the PVP–PI and PVP–$(PI)_x$ copolymers were prepared with a previously reported method:[6] Grade No. 4 ASTM V-2, clear and slightly stained Muscovite, ruby red mica (Asheville-Schoonmaker Mica Co.) was used as the substrate. Two (or four) freshly cleaved, atomically smooth mica sheets of identical thicknesses (in a range 1–3 μm), being silvered at one side, were prepared for each run of the symmetric (or asymmetric) adhesion experiments. The mica sheets (with area ≅ 1 cm^2) were pasted with a standard *sugar glue* (glucose/galactose 50/50 mixture) at their silvered side on fused silica cylindrical lenses (of radius = 1 or 2 cm), and the copolymers were adsorbed on these sheets at 20 °C from toluene solutions (≅300 mL in volume) of concentration =2–3 $\mu g/cm^3$ in clean glass jars. Guaranteed grade toluene (Wako) was used after filtration without further purification. The adsorbed amount was quite insensitive to the solution concentration in this range.

After the adsorption was saturated (within 6 h), the lenses and mica sheets bearing the adsorbed copolymers were soaked in pure toluene (≅300 mL in volume) for several times (each for 2 h) to remove all nonadsorbed copolymers, and thoroughly dried by passing clean nitrogen gas through the glass jars for more than 12 h. No desorption takes place during this procedure.[6,11] Previous studies[11,17] indicate that molecularly smooth, very thin, dry adsorbed copolymer layers having PVP blocks at the bottom and PI blocks at the top are prepared with the method used in this study.

Mechanical Measurements. For the dry, adsorbed layers of the PVP–PI and PVP–$(PI)_x$ copolymers, adhesive forces were measured at 20 °C with a laboratory-made apparatus. In this apparatus, two cylindrical lenses each bearing the mica sheet were mounted in a face-to-face cross-cylinder geometry: As schematically shown in Figure 1, an upper lens (L_u) was fixed at the apparatus frame (F), and a lower lens (L_l) was mounted on a double-leaf spring (S; stiffness $\kappa = 2.8 \times 10^5$ dyn/cm) being supported by a micrometer-driven shaft (D). The copolymer layers on the mica sheets were brought toward contact and separated by pushing the shaft up and down. Basic structure and operation of our adhesive force apparatus were similar to those of the Israelachvili type surface-force apparatus (SFA),[18] but differing from the SFA used in a previous adhesion study,[6] our apparatus measured forces with a calibrated differential transducer (pair of strain gauges; T shown in Figure 1) attached to the spring.

Figure 1 shows a typical transducer output (∝force between copolymer layers) and bend of the spring during an adhesion experiment. At point a, the layers were far apart and the output was on the zero-force base line. On approach of the layers, an adhesive jump spontaneously took place at point b to generate a positive output that indicated a tensile load on the layers due to the spring bend. When necessary (not the case in Figure 1), optical measurements explained below were carried out at this point. Then, up to point c, a small compressive load detected as the negative output was applied by pushing up the shaft. With this operation, the contact spot area became *slightly* larger than that at zero load and faster equilibration of adhesion was achieved. The compressive load was kept smaller than 200 dyn so as to avoid plastic deformation of the sugar glue. After point c, the shaft was pushed down and an increasing tensile load was slowly applied to the layers. At point d, the layers jumped apart due to the action of the spring and the output returned to zero. An adhesive

Table 2. Characteristics of PVP–$(PI)_x$ Graft-Block Copolymers[a]

	graft-block copolymers			PVP prepolymer (trunk)		PI prepolymer (branch)	
code[b]	$10^{-3}M$[c]	M_w/M_n	$10^{-3}M_{span}$[d]	$10^{-3}M$[c]	M_w/M_n	$10^{-3}M$[c]	M_w/M_n
PVP–$(PI)_x$ 32–$(18)_{13}$	262	1.15	2.5	32.0	1.06	17.6	1.04
PVP–$(PI)_x$ 80–$(18)_{40}$	777	1.13	2.0	79.7	1.06	17.6	1.04

[a] PI microstructure: cis/trans/vinyl ≅ 75/20/5.[16] [b] x indicates the number of PI branches per copolymer chain. [c] Weight-average molecular weight. [d] Average molecular weight of the PVP span between neighboring PI branches.

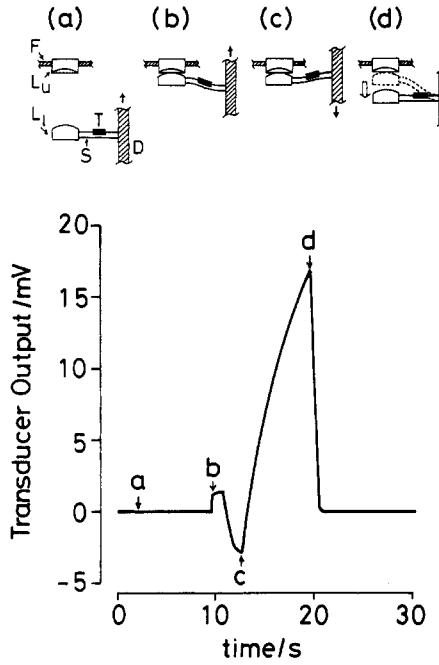

Figure 1. Example of the force-transducer output obtained during a symmetric adhesion experiment for the PVP–PI 102–164 copolymer layer. Positive and negative outputs indicate tensile and compressive loads, respectively. The corresponding bend of the double-leaf spring is also shown schematically. Key: L_u and L_l, upper and lower lenses on which mica sheets bearing adsorbed copolymers are pasted; F, frame of the adhesive force apparatus; D, micrometer-driven shaft; T, force-transducer (pair of strain gauges) attached to the double-leaf spring (S).

force (pull-off force necessary to separate the layers), F_a, was evaluated from the output at this point.

All measurements were carried out for circular contact spots. F_a was measured repeatedly and reproducibly for the same contact spot, indicating that the adsorbed layers were not damaged during the above experimental procedure. In each run of the measurements, F_a was measured for several different contact spots and the resulting F_a values agreed well. The F_a values were quite insensitive to the tensile load increasing rate (from point c to d shown in Figure 1) and also to the compressive load level (<200 dyn) and the holding time at point c. These results correspond to a previous observation that F_a was independent of a contact time,[6] meaning that F_a reflects a surface free energy at equilibrium and has no kinetic contribution (like viscoelastic relaxation of PI blocks). For such cases, previous studies[6,19,20] indicated the validity of the Johnson–Kendall–Roberts (JKR) theory[21] of adhesive contact mechanics. Thus, as before,[6] we used this theory to evaluate the adhesion energy per unit area (surface free energy decrease on contact) as

$$\gamma = F_a/3\pi R \tag{1}$$

Here, R is a radius of surface curvature for the two copolymer layers.[21] Around the contact spot the surface profile for the layers is equivalent to that for a sphere being in contact with a flat plane, and R was evaluated from optical measurements explained below.

For adhesion between identical copolymer layers (referred to as *symmetric* adhesion) and between different copolymer layers (*asymmetric* adhesion), γ was determined at 20 °C from several independent experiments, each using freshly prepared mica sheets and solutions. For the layers used in the asymmetric adhesion experiments, γ for symmetric adhesion was also measured as a control and good reproducibility was found. (Those control experiments required four mica sheets of identical thicknesses, two for each copolymer.)

The JKR theory enables us to evaluate γ also from the dependence of the contact spot diameter d on the applied load P *if the system (including the surfaces and substrates) deforms elastically with the load.*[21] In fact, Creton, Brown, and Shull[12] examined this dependence in their adhesion experiments for thin PS–PI block copolymer layers and elastically deforming rubber lenses (cross-linked PI). *In principle*, γ can be evaluated from the P dependence of d also for our PVP–PI layers. However, the sugar glue used in our experiments exhibited plastic deformation for large P (>200 dyn),[22] as explained below in relation to the optical measurements. For this case, the JKR theory could not be applied. On the other hand, for small P (<200 dyn) the glue deformed elastically but d remained close to the zero-load contact diameter (=0.05–0.1 mm). Thus, for our copolymer layers, the γ values were determined from F_a (after imposition of small P), not from the P dependence of d.

Optical Measurements. Due to optical interference between the silvered layers (half-mirrors) at the back of the mica sheets, fringes of equal chromatic order were observed when a white light beam was passed through the sheets in our adhesive force apparatus. The fringes exhibited characteristics of strong adhesion of the adsorbed copolymers, spontaneous flattening of the fringe head on close approach of the surfaces, the head wavelength being independent of the applied load, and non-zero width of the flat fringe head at jump (point d in Figure 1). When the compressive load P (at point c in Figure 1) exceeded 200 dyn, a portion of the fringe head remained flat even after the surfaces jumped apart. This behavior was indicative of plastic deformation of the sugar glue.[22] Thus, P was kept smaller than 200 dyn for all measurements. For those small P, the sugar glue deformed elastically and the fringe head recovered its round shape after the jump.

When the two copolymer layers jumped into adhesive contact, wavelengths of the flat fringe head (for the contact spot) were measured with a spectrometer (JASCO CT-25 CX). Those wavelengths were analyzed according to the interference formulas of Israelachvili[23] to evaluate the adsorbed layer thickness, L. (The analysis required wavelengths for bare mica contact, that were determined before the copolymers were adsorbed.) Wavelengths were measured and analyzed also for five to seven points in the fringe tails (out of the contact spot) to evaluate the surface separation h as a function of the distance ϱ from the central axis of the contact spot (cf. Figure 7 of ref 6). For intermediate h values typically in a range 2000 Å < h < 5000 Å, the resulting $h-\varrho$ profiles were well fit with a profile for a sphere being in contact with a flat plane, $h = R - [R^2 - \varrho^2]^{1/2}$ + const $\cong \varrho^2/2R$ + const (for $\varrho \ll R$) with R = sphere radius. The R value for the copolymer layers before contact, being preserved in that range of h after contact, was evaluated from this fit. (In a closer neighborhood of the contact spot with smaller h, the profile was distorted from the sphere profile due to strong adhesion.)

III. Results and Discussion

III-1. Adsorption Density. Table 3 summarizes the thickness L and the PI block adsorption density σ_{PI} (=*number* of the PI blocks per unit area) for the dry, adsorbed copolymer layers examined:

$$\sigma_{PI} = \frac{xLN_A}{M}\left[\frac{\phi_{PVP}}{d_{PVP}} + \frac{\phi_{PI}}{d_{PI}}\right]^{-1} \tag{2}$$

Here, x is the number of PI blocks per copolymer ($x = 1$ for the diblock copolymers), M is the copolymer molecular weight, N_A is the Avogadro number, and ϕ_B and d_B are the content in the copolymer and density of the block B (=PVP, PI), respectively. Obviously, σ_{PI} was determined when the copolymers were adsorbed *in toluene* to form polymer brushes.

Parsonage et al.[11] examined adsorption of PVP–PI and PVP–PS diblock copolymers on mica in toluene at 32 °C and measured the adsorption densities σ_{brush} for the brush blocks (=PI, PS). They found a universal relationship between reduced quantities, a normalized

Table 3. Characteristics of Dry Block Copolymer Layers Adsorbed on Mica

copolymer	L (Å)	$10^{-12}\sigma_{PI}$[a] (chains/cm^2)	γ[b] (erg/cm^2)	$\Delta\gamma$[c] (erg/cm^2)	$R_{\theta,PI}/L_{PI}$
PVP–PI Diblock Copolymers					
PVP–PI 1–18	14	4.2	51	19	8.0
PVP–PI 49–32	22	1.7	48	16	15.1
PVP–PI 15–73	26	1.7	66	34	10.0
PVP–PI 34–73	25	1.4	70	38	12.1
PVP–PI 72–73	18	0.72	69	37	22.9
PVP–PI 102–164	26	0.58	50	18	19.2
PVP–PI 72–338	20	0.28	55	23	27.6
PVP–(PI)$_x$ Graft-Block Copolymers					
PVP–(PI)$_x$ 32–(18)$_{13}$	19	5.2	53	21	6.5
PVP–(PI)$_x$ 80–(18)$_{40}$	26	7.5	43	11	4.5

[a] Number of PI blocks in a unit area of a layer; $2\sigma_{PI}$ chains exist in a unit area of two layers in contact. [b] Adhesion energy per unit area for the symmetric contact at 20 °C. [c] Extra adhesion energy per unit area at 20 °C: $\Delta\gamma = \gamma - \gamma_{homo\text{-}PI}$ ($\gamma_{homo\text{-}PI}$ = 32 erg/cm^2).[26]

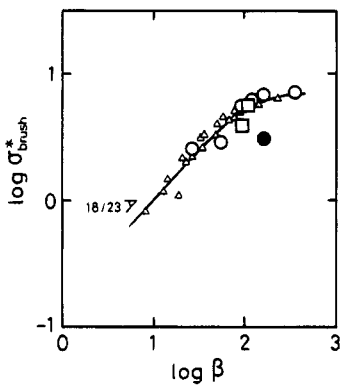

Figure 2. Plots of the reduced adsorption density for the brush blocks σ_{brush}* against the asymmetry ratio β. The circles and squares indicate σ_{brush}* for the PVP–PI diblock and PVP–(PI)$_x$ graft-block copolymers examined in this study. Those copolymers were adsorbed on mica from toluene solutions at 20 °C. The σ_{brush}* data obtained by Parsonage et al.[11] for PVP–PI and PVP–PS diblock copolymers adsorbed at 32 °C are multiplied by a factor 1.35 and shown by the triangles.

adsorption density $\sigma_{brush}^* = \sigma_{brush}\pi S_{brush}^2$ and an asymmetry ratio $\beta = N_{brush}^{6/5}/N_{PVP}^{2/3}$ (cf. triangles in Figure 2). Here, S_{brush} and N_{brush} are the radius of gyration in toluene and degree of polymerization for the brush block and N_{PVP} is the degree of polymerization of the anchoring PVP block. σ_{brush}* is a measure for the crowdedness in the brush layers, and β is related to a balance of the brush free energy and van der Waals attraction between the PVP block and mica. As discussed by Parsonage et al.,[11] the universal σ_{brush}^*–β relationship suggests that the adsorbed amount is thermodynamically determined. In fact, they found a power-law relationship, $\sigma_{brush}^* \propto \beta^{18/23}$ for small β.[11] This relationship is in agreement with the Marques–Joanny–Leibler (MJL) theory[24] for equilibrium adsorption.

Here, it is interesting to examine whether the comb-shaped graft-block copolymers used in this study obey the same thermodynamics of adsorption (in toluene) as the linear diblock copolymers do. For the PVP–PI diblock copolymers, we used the data in Table 3 to evaluate σ_{brush}* (σ_{PI}*) and β according to the definition of Parsonage et al.[11] For the PVP–(PI)$_x$ graft-block copolymers, we equally divided the PVP trunk to each PI branch and evaluated σ_{brush}* and β for the resulting hypothetical PVP–PI diblock copolymer having the PVP and PI blocks of molecular weights M_{span} and M_{PI} (cf. Table 2). This definition of σ_{brush}* and β for the graft-block copolymers is naturally derived from the MJL theory.[24]

Figure 2 shows plots of σ_{brush}* against β. Circles and squares indicate the σ_{brush}* data obtained in this study for the diblock and graft-block copolymers, respectively. The σ_{brush}* values obtained by Parsonage et al.[11] were 30–40% smaller than our values except for the PVP–PI 1–18 copolymer (filled circle). Thus, their σ_{brush}* were multiplied by a factor 1.35 and shown with the triangles in Figure 2. As seen there, the β dependence of σ_{brush}* agrees well for their and our data (except for PVP–PI 1–18). This result suggests that the diblock and graft-block copolymers examined in this study obey the same thermodynamics of adsorption that was discussed in detail by Parsonage et al.[11]

The difference in magnitude of our and their σ_{brush}* data (not in the β dependence) can be explained as follows. As considered in the MJL theory,[24] the adsorption equilibrium is essentially determined by a balance of the brush free energy and the van der Waals attraction between the PVP block layer and mica. This attraction is reduced and σ_{brush}* is decreased when the PVP blocks are swollen with toluene. The copolymers were adsorbed at 20 °C in our experiments, while at a higher temperature, 32 °C, in the experiments of Parsonage et al.[11] Thus, the PVP blocks should be more swollen and σ_{brush}* is smaller in their experiments. In relation to this argument, the considerably small σ_{brush}* value of our PVP–PI 1–18 copolymer (filled circle in Figure 2) can be attributed to its very short PVP block (M_{PVP} = 1.1k) that should be largely swollen with toluene even at 20 °C. It should be also noted that the two graft-block copolymers (squares) having short PVP spans (M_{span} = 2.5k and 2k) do not exhibit such small σ_{brush}* values because the PVP trunks themselves are sufficiently long (M_{PVP} = 32k and 80k) and little swollen with toluene at 20 °C.

III-2. Symmetric Adhesion Energy. The adhesion energies per unit area, γ (at 20 °C), have been summarized in Table 3 for *symmetric* contact of the dry, adsorbed copolymer layers: γ reflects the interaction of the PI blocks located at the top of the layers. For comparison, ratios of the unperturbed end-to-end distances $R_{\theta,PI}$ of the PI blocks (evaluated from literature data[25]) to the PI layer thicknesses L_{PI} (evaluated from the σ_{PI} and M_{PI} data) are also shown.

As seen in Table 3, the $R_{\theta,PI}/L_{PI}$ ratios are significantly larger than unity, meaning that the PI blocks are forced to take highly flattened conformations in the dry, adsorbed layers. Corresponding to this flattened conformation, γ of the PI blocks is larger than the surface energy per unit area of homo-PI films of macroscopic size, $\gamma_{homo\text{-}PI}$ = 32 erg/cm^2 (at 20 °C).[26] $\gamma_{homo\text{-}PI}$ is regarded as the van der Waals contribution to the adhesion energy, and the extra adhesion energy for the PI blocks, $\Delta\gamma = \gamma - \gamma_{homo\text{-}PI}$, can be related to their flattened conformation:[6] As explained earlier, the flattened PI blocks belonging to each layer should interpenetrate each other to increase their conformational entropy, and $\Delta\gamma$ has been attributed to this entropy gain (decrease of the elastic free energy).[6]

As seen in Table 3, $\Delta\gamma$ varies with the molecular weight M_{PI} and adsorption density σ_{PI} of the PI block. We here examine whether this M_{PI} and σ_{PI} dependence can be explained from the above mechanism of extra adhesion. For this purpose, we consider ideal, tethered chains confined in a layer of thickness $L_{PI} \ll R_\theta$ (unperturbed end-to-end distance of the chain). The

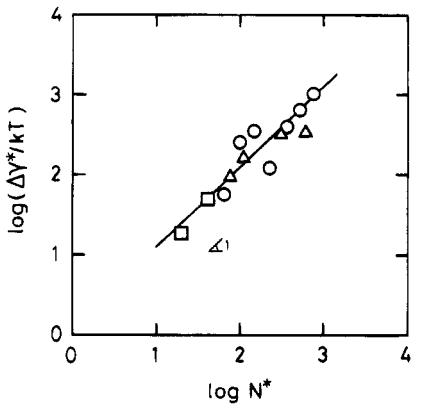

Figure 3. Plots of the extra adhesion energy per PI block reduced by the thermal energy, $\Delta\gamma^*/kT$ (T = 293 K), against the PI block length *normalized by the layer thickness*, N^* (cf. eqs 5 and 8). The circles and squares indicate $\Delta\gamma^*/kT$ for symmetric contact of the PVP–PI diblock and PVP–$(PI)_x$ graft-block copolymers, respectively, and the triangles indicate $\Delta\gamma^*/kT$ for asymmetric contact of the PVP–PI diblock copolymers. The solid line indicates a relationship, $\Delta\gamma^* = (\pi^2/8)N^*kT$ (cf. eq 4).

elastic free energy of the chain, $f(L_{PI})$, can be calculated with a standard method[27-30] described in the Appendix. As shown there, each chain has

$$f(L_{PI}) = (\pi^2kT/6)(R_\theta/L_{PI})^2 + kT \ln L_{PI} + f_0 \quad (\text{for } L_{PI} \ll R_\theta) \quad (3)$$

Here, f_0 is a constant independent of L_{PI} and kT is the thermal energy. On contact of the two identical layers, the chain belonging to one layer can interpenetrate into the other and decrease its free energy by a factor

$$\Delta\gamma^* = f(L_{PI}) - f(2L_{PI}) = (\pi^2/8)N^*kT \quad (\text{for } N^* \gg 1) \quad (4)$$

with

$$N^* = (R_\theta/L_{PI})^2 \quad (5)$$

Here we have neglected a term involved in $\Delta\gamma^*$ (eq 4), $-kT \ln 2$, that is much smaller than the leading term, $(\pi^2/8)N^*kT$. (The copolymer layers had $N^* > 20$.)

The PI blocks confined in the thin layer are subjected to an osmotic requirement of uniform segment density. Thus, the term f_0 involved in eq 3 should be different for the PI blocks and the ideal chains (not subjected to this requirement). However, for $L_{PI} \ll R_\theta$, the L_{PI} dependent part of $f(L_{PI})$ would be hardly affected by this requirement and eq 4 would give a good approximation for the free energy decrease due to interpenetration of the PI block.

Equation 4 predicts a universal proportionality between the extra adhesion energy *per PI block*, $\Delta\gamma^* = \Delta\gamma/2\sigma_{PI}$ ($2\sigma_{PI}$ blocks exist in the two layers), and the block length normalized by the layer thickness, N^*, irrespective of the σ_{PI}, M_{PI}, and L_{PI} values. For a test of this prediction, we evaluated $\Delta\gamma^*/kT$ and N^* from the data in Table 3 and examined their relationship. The results are shown in Figure 3 by the circles (for the diblock copolymers) and squares (for the graft-block copolymers). We note that the data for those copolymers are collapsed around the solid line that represents the relationship given by eq 4: The observed proportionality between $\Delta\gamma^*$ and N^*kT is in accordance with eq 4, and the magnitude of $\Delta\gamma^*$ is also described satisfactorily.

Table 4. Adhesion Energy for Asymmetric Contact of Two Copolymer Layers at 20 °C

copolymer layers	γ (erg/cm^2)	$\Delta\gamma^a$ (erg/cm^2)
PVP–PI 1–18 & PVP–PI 15–73	55	23
PVP–PI 1–18 & PVP–PI 72–338	62	30
PVP–PI 49–32 & PVP–PI 72–338	58	26
PVP–PI 72–73 & PVP–PI 72–338	46	14

[a] Extra adhesion energy per unit area for asymmetric contact: $\Delta\gamma = \gamma - \gamma_{homo\text{-}PI}$ ($\gamma_{homo\text{-}PI}$ = 32 erg/cm^2).[26]

This result strongly suggests that the extra adhesion of the adsorbed copolymer layers is due to the conformational entropy gain on contact of flattened PI blocks.

III-3. Asymmetric Adhesion Energy. Table 4 summarizes the adhesion energy per unit area, γ, for asymmetric contact of different diblock copolymer layers. Clearly, γ is larger than the van der Waals contribution, $\gamma_{homo\text{-}PI}$ = 32 erg/cm^2, as was the case also for the symmetric adhesion. We here examine whether the extra adhesion energies $\Delta\gamma$ ($=\gamma - \gamma_{homo\text{-}PI}$) for the asymmetric and symmetric contacts are consistently explained from the mechanism considering the conformational entropy gain on contact.

We consider two layers of ideal, tethered chains 1 and 2 having thicknesses L_1 and L_2 and adsorption densities σ_1 and σ_2, respectively. On the asymmetric contact, the layer thickness available for chain 1 is increased from L_1 to $L_1 + L_2$, and the elastic free energy decrease per chain 1 is given by (cf. eq 3)

$$\Delta\gamma^*_1 = [\pi^2kTR_{\theta,1}{}^2/6][L_1{}^{-2} - (L_1 + L_2)^{-2}] \quad (6)$$

Similarly, for chain 2 the free energy decrease is

$$\Delta\gamma^*_2 = [\pi^2kTR_{\theta,2}{}^2/6][L_2{}^{-2} - (L_1 + L_2)^{-2}] \quad (7)$$

The adhesion energy averaged for chains 1 and 2 is $\Delta\gamma^* = [\sigma_1\Delta\gamma^*_1 + \sigma_2\Delta\gamma^*_2]/[\sigma_1 + \sigma_2]$. (As done in eq 4, small additional terms involved in $\Delta\gamma^*_i$, $kT \ln[L_i/(L_1 + L_2)]$ (i = 1, 2), have been neglected in eqs 6 and 7.)

From eqs 6 and 7, eq 4 is expected to hold for both cases of asymmetric and symmetric contacts *if the normalized chain length is redefined as*

$$N^* = [4\phi_1R_{\theta,1}{}^2/3][L_1{}^{-2} - (L_1 + L_2)^{-2}] + [4\phi_2R_{\theta,2}{}^2/3][L_2{}^{-2} - (L_1 + L_2)^{-2}] \quad (8)$$

with $\phi_i = \sigma_i/[\sigma_1 + \sigma_2]$ (i = 1, 2). For the symmetric contact, this definition is reduced to eq 5. As a test for this expectation, $\Delta\gamma^*$ ($=\Delta\gamma/[\sigma_1 + \sigma_2]$) and N^* (eq 8) for the asymmetric adhesion were evaluated from the data in Tables 3 and 4. The resulting $\Delta\gamma^*$ *vs* N^* plots have been shown in Figure 3 by the triangles. As seen there, the data for the asymmetric adhesion are well superposed on the data for the symmetric adhesion (circles and squares) and closely obey eq 4. This result agrees with the above expectation, again supporting the validity of the above mechanism of extra adhesion.

III-4. Comparison with Other Asymmetric Adhesion Data. Recently, Creton, Brown, and Shull studied the fracture toughness of interfaces between cross-linked PI networks of macroscopic size and thin PS–PI diblock copolymer layers having the PI blocks at the top.[12] The toughness, G, is enhanced by the PI blocks that interpenetrate into the network on contact. This situation is similar to that for the adhesion of the adsorbed PVP–PI copolymer layers examined in this paper.

Creton, Brown, and Shull found that G increases from a threshold value, G_0, first very rapidly and then slowly with increasing crack-propagating velocity V, and that G_0 monotonically increases with the surface density σ_{PI} and the degree of polymerization N of the PI blocks.[12] They attributed the rapid increase of G at low V to a very long characteristic time for pulling out the PI blocks from the network, and the slow increase of G at high V to viscoelastic bulk losses.[12] In a static state ($V = 0$), these kinetic contributions vanish and the remaining G_0 determines the fracture behavior. Thus, G_0 is similar in nature to the adhesion energy γ studied here in a sense that both G_0 and γ represent the static effect(s) of the PI blocks on adhesion.

The ranges of σ_{PI} and M_{PI} are similar for our PVP–PI layers and the PS–PI layers examined by Creton, Brown, and Shull.[12] Nevertheless, γ for PVP–PI is significantly smaller than G_0 for PS–PI: For example, for our PVP–PI 102–164 layer we have $\gamma = 4.3 \times 10^{-11}$ erg *per PI block* (cf. Table 3), while for the PS–PI layer of nearly the same σ_{PI} and M_{PI} (=150k) we find $G_0 \cong 40 \times 10^{-11}$ erg *per PI block* (cf. Figure 4b of ref 12). This order-of-magnitude difference between γ and G_0 naturally suggests a difference in the adhesion mechanism for the PVP–PI layers and the PS–PI/PI network system.

The G_0 data for the latter system[12] were explained from the Raphaël–de Gennes theory.[13,14] For adhesion of two rubbery films 1 and 2, the former having tethered chains at its surface and the latter being subjected to the interpenetration of those chains, the theory considers that the tethered chains embedded in film 2 are pulled out and stretched (in air) on the interfacial frature. (The conformational entropy gain on contact of flattened chains is not considered in the theory.) This stretched-chain pullout mechanism requires an extra energy for the fracture and enhances the fracture toughness. From the above difference between γ and G_0, we expect that this mechanism being valid for the PS–PI/PI network systems is not the mechanism enhancing the adhesion of the PVP–PI layers. This expectation is examined below.

For the symmetric and asymmetric contacts of the PVP–PI layers, the extra adhesion energy per PI block deduced from the Raphaël–de Gennes theory is written as

$$\Delta\gamma^* \propto NkT \tag{9}$$

Here, $N = (\sigma_1 N_1 + \sigma_2 N_2)/(\sigma_1 + \sigma_2)$ is a number-average degree of polymerization of the PI blocks in layers 1 and 2. Equation 9 is similar to eq 4, except that N^* in eq 4 is the PI block length *normalized by the PI layer thickness* L_{PI} (cf. eqs 5 and 8).

The validity of eq 9 is tested in Figure 4 where $\Delta\gamma^*/kT$ is plotted against N for the PVP–PI layers. The filled and unfilled symbols indicate the data for the asymmetric and symmetric adhesion, respectively. The Raphaël–de Gennes theory (eq 9) predicts that $\Delta\gamma^*/kT$ is proportional to N but *independent* of L_{PI}. However, the $\Delta\gamma^*/kT$ *vs* N plots are scattered, and $\Delta\gamma^*/kT$ systematically *decreases* with increasing L_{PI} for the symmetric adhesion of the PVP–PI layers having the *same* N (see the inserted figure). These results indicate that the extra adhesion of the adsorbed PVP–PI layers is not due to the stretched-chain pullout mechanism, as expected above. Instead, as seen from Figure 3, the adhesion of those layers is quite possibly dominated by the conformational entropy gain for the flattened PI blocks.

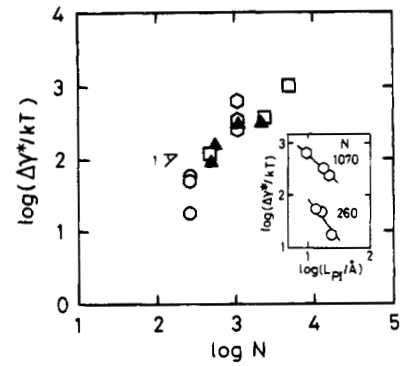

Figure 4. Plots of the extra adhesion energy per PI block reduced by the thermal energy, $\Delta\gamma^*/kT$ (T = 293 K), against the (number-average) degree of polymerization of the PI block, N. Filled and unfilled symbols indicate the data obtained for the asymmetric and symmetric contacts, respectively. For the symmetric adhesion: circles, for copolymers including a PI block of N = 260 (M_{PI} = 17.6k); hexagons, for copolymers including a PI block of N = 1070 (M_{PI} = 73k); squares, for other copolymers (cf. Tables 1 and 2). The inserted figure indicates the L_{PI} dependence of $\Delta\gamma^*/kT$ for the symmetric adhesion at constant N (=260 and/or 1070).

For the stretched-chain pullout mechanism to be valid, the tethered chain (PI blocks) being pulled out from a rubbery film (PI network or PVP–PI layer) should be firmly gripped at its portion remaining in the film. This situation would have been realized for the PI networks of *macroscopic size*, leading to the agreement between the G_0 data and the Raphaël–de Gennes theory.[12] On the other hand, the adsorbed PVP–PI copolymer layers are *very thin* (cf. Table 3) and would have failed to grip the interpenetrating PI blocks even when the blocks are only partially pulled out. For this case, the conformational entropy gain dominates the enhanced adhesion. Thus, the difference in the size (thickness) of the bulk PI network and thin PVP–PI layers seems to have led to the significant difference between G_0 and γ ($\ll G_0$).[31]

Finally, we would like add a comment for an experimental test that can distinguish the two adhesion mechanisms, conformational entropy gain and the stretched-chain pullout. As explained earlier, the adhesion energy γ can be determined with two methods, one by measuring the pull-off force F_a (eq 1) and the other by measuring the contact spot diameter d as a function of the applied load P. If the stretched-chain pullout mechanism is dominant, γ determined with the second method would exhibit hysteresis on imposition of tensile and compressive loads. On the other hand, no hysteresis is expected if the conformational entropy gain dominates γ. In this study, the second method could not be used because of the plastic deformation of the sugar glue (for large P). However, if we could modify our experimental setup either by mechanically holding the mica sheets (without using glue) or by using some elastically deforming, toluene-insoluble glue instead of the sugar glue, we would be able to evaluate γ for the adsorbed PVP–PI layers with the second method and directly examine the contribution of the stretched-chain pullout mechanism to γ. This is considered as interesting future work.

IV. Concluding Remarks

As discussed in Figures 3 and 4, the extra adhesion for dry, adsorbed PVP–PI and PVP–$(PI)_x$ copolymer layers is quite possibly due to the interpenetration and the resulting conformational entropy gain of the PI

blocks on contact, not due to the stretched-chain pullout mechanism. It should be emphasized that this entropy gain emerges only for contact of layers of *flattened* chains in the *rubbery state*, not for contact of glassy layers (such as PVP–PS layers) or layers of the thickness $L \geq R_\theta$ (for which interpenetration does not significantly increase the conformational freedom). For further investigation of the mechanism of enhanced adhesion, it is interesting to study the temperature dependence of $\Delta\gamma$ and examine if $\Delta\gamma$ has an entropic origin ($\Delta\gamma \propto T$). It is also interesting to study the L dependence of $\Delta\gamma$ for adhesion of two layers in a wide range of L and examine if the stretched-chain pullout mechanism becomes dominant for large L ($\geq R_\theta$). These issues deserve further attention.

Acknowledgment. We acknowledge with thanks an important comment from a reviewer for this paper about the difference between the two adhesion mechanisms discussed in section III-4. We acknowledge with thanks financial support from the Ministry of Education, Science, and Culture, Japan, under Grant No. 03750650.

Appendix: Elastic Free Energy of Confined Tethered Chain

We consider ideal chains confined in a thin layer between two infinitely large, impermeable walls located at positions $x = 0$ and L. These chains are tethered on the wall at $x = 0$, and the layer thickness L is assumed to be much smaller than the unperturbed end-to-end distance $R_\theta = bN^{1/2}$ (b = segment step length, N = degree of polymerization).

In a continuous limit, the distribution function for the nth segment, $W(\mathbf{r},n)$ with $\mathbf{r} = (x, y, z)$, is described by a standard diffusion equation,[27-30]

$$\frac{\partial}{\partial n}W(\mathbf{r},n) = \frac{b^2}{6}\frac{\partial^2}{\partial \mathbf{r}^2}W(\mathbf{r},n) \tag{A1}$$

The boundary condition representing the wall effect is written as[27-30]

$$W|_{x=0} = W|_{x=L} = 0 \qquad (\text{for } n > 0) \tag{A2}$$

The initial condition is

$$W(\mathbf{r},0) = \delta(\mathbf{r} - \mathbf{r}_0) \qquad (\text{for } 0 < x < L) \tag{A3}$$

with $\mathbf{r}_0 = (x_0, y_0, z_0)$ being the location of the tethered end of the chain. Obviously, $x_0 = 0$ for the chain tethered on the wall. However, for a moment, we leave x_0 as a free parameter. Then, eq A1 is solved as

$$W(\mathbf{r},n) = w_x(x,n)\, w_y(y,n)\, w_z(z,n) \tag{A4}$$

with

$$w_\xi(\xi,n) = \left[\frac{2\pi b^2 n}{3}\right]^{-1/2} \exp\left\{-\frac{3(\xi - \xi_0)^2}{2b^2 n}\right\} \qquad (\xi = y, z) \tag{A5}$$

and

$$w_x(x,n) = \left[\frac{2\pi b^2 n}{3}\right]^{-1/2} \sum_{p=-\infty}^{\infty}\left[\exp\left\{-\frac{3(x - x_0 - 2pL)^2}{2b^2 n}\right\} - \exp\left\{-\frac{3(x + x_0 - 2pL)^2}{2b^2 n}\right\}\right] \tag{A6}$$

(For obtaining this w_x, we have placed positive and negative sources (delta functions) at $x = x_0 \pm 2pL$ (p = 1, 2, ...) and $x = -x_0 \pm 2pL$ (p = 0, 1, 2, ...) so that the boundary condition is satisfied.[27])

Now, we allow x_0 to approach 0 so that the tethered end is located on the wall. For $x_0 \to 0$, eq A6 becomes

$$w_x(x,n) \propto \left[\frac{2\pi b^2 n}{3}\right]^{-3/2} \sum_{p=-\infty}^{\infty}(x - 2pL) \times \exp\left\{-\frac{3(x - 2pL)^2}{2b^2 n}\right\} \tag{A7}$$

The elastic free energy of the chain, $f(L)$, is calculated from $W(\mathbf{r},N)$ as[28-30]

$$f(L) = -kT \ln[\int_0^L w_x(x,N)\, dx \int_{-\infty}^{\infty} w_y(y,N)\, dy \times \int_{-\infty}^{\infty} w_z(z,N)\, dz] = C - kT \ln H(L) \tag{A8}$$

with C being an L-independent constant and H being given by

$$H(L) = 2\vartheta(6L^2/\pi R_\theta^2) - \vartheta(3L^2/2\pi R_\theta^2) \tag{A9}$$

Here, $\vartheta(\xi)$ is the theta series defined by[32]

$$\vartheta(\xi) = \sum_{p=-\infty}^{\infty} \exp(-p^2\pi\xi) \tag{A10}$$

Using a relationship valid for this series,[32] $\vartheta(\xi) = \xi^{-1/2}\vartheta(1/\xi)$, we can rewrite $H(L)$ as

$$H(L) = \frac{2}{L}\left[\frac{2\pi R_\theta^2}{3}\right]^{1/2} \sum_{p=1}^{\infty}\left[\exp\left\{-\frac{\pi^2 R_\theta^2 p^2}{6L^2}\right\} - \exp\left\{-\frac{2\pi^2 R_\theta^2 p^2}{3L^2}\right\}\right] \tag{A11}$$

For the thin layer (with $L \ll R_\theta$) considered here, the sum in eq A11 is dominated by a term, $\exp[-\pi^2 R_\theta^2 p^2/6L^2]$ with $p = 1$. Then, from eqs A8 and A11, we finally obtain

$$f(L) = (\pi^2 kT/6)(R_\theta/L)^2 + kT \ln L + f_0 \tag{A12}$$

with f_0 being a constant independent of L. This final result does not depend on the location x_0 of the tethered end if $0 < x_0 \ll L$: Instead of eq A7, a standard Fourier series expression of $w_x(x,n)$ is obtained for this case:[28-30]

$$w_x(x,n) = \frac{2}{L}\sum_{p=1}^{\infty} \sin\frac{p\pi x}{L} \sin\frac{p\pi x_0}{L} \exp[-p^2\pi^2 nb^2/6L^2] \tag{A13}$$

Considering the condition $0 < x_0 \ll L \ll R_\theta$, we can easily obtain eq A12 from eq A13.

On symmetric contact of two identical layers, $f(L)$ decreases by a factor $\Delta\gamma^* = f(L) - f(2L) = (\pi^2/8)N^*kT$ wit $N^* = (R_\theta/L)^2$ (cf. eq A12). (For large N^* a term, $-kT$ ln 2, involved in $\Delta\gamma^*$ is negligibly small as compared to the leading term, $(\pi^2/8)N^*kT$.) This proportionality between $\Delta\gamma^*$ and N^* is found also from a very simple argument: We regard the tethered chain as a planar chain that is composed of N^* blobs of size L and placed on a 2-dimensional lattice of coordination number z. On contact, the lattice becomes double layered and the coordination number is increased from z to z'. Then, the number of the chain conformation is increased from $\Omega = \omega_{blob}z^{N^*}$ to $\Omega' = \omega_{blob}(z')^{N^*}$, with ω_{blob} being the conformational freedom in each blob, and the resulting elastic free energy decrease, $\Delta\gamma^* = kT$ ln (Ω'/Ω), is proportional to N^*kT.

References and Notes

(1) Halperin, A.; Tirrell, M.; Lodge, T. P. *Adv. Polym. Sci.* **1992**, *100*, 31.
(2) Patel, S.; Tirrell, M. *Annu. Rev. Phys. Chem.* **1989**, *40*, 597.
(3) See, for example: Napper, D. *Polymeric Stabilization of Colloidal Dispersions*; Academic Press: London, 1983.
(4) Hadziioannou, G.; Patel, S.; Granick, S.; Tirrell, M. *J. Am. Chem. Soc.* **1986**, *108*, 2869.
(5) Patel, S.; Tirrell, M.; Hadziioannou, G. *Colloid Surf.* **1988**, *31*, 157.
(6) Watanabe, H.; Tirrell, M. *Macromolecules* **1993**, *26*, 6455.
(7) Dhoot, S.; Watanabe, H.; Tirrell, M. *Colloid Surf. A* **1994**, *86*, 47.
(8) Taunton, H. J.; Toprakcioglu, C.; Fetters, L. J.; Klein, J. *Nature* **1988**, *332*, 712; *Macromolecules* **1990**, *23*, 571.
(9) Taunton, H. J.; Toprakcioglu, C.; Klein, J. *Macromolecules* **1988**, *21*, 3333.
(10) Milner, S. T.; Witten, T. A.; Cates, M. E. *Macromolecules* **1988**, *21*, 2610; *Europhys. Lett.* **1988**, *5*, 413.
(11) Parsonage, E.; Tirrell, M.; Watanabe, H.; Nuzzo, R. *Macromolecules* **1991**, *24*, 1987.
(12) Creton, C.; Brown, H. R.; Shull, K. R. *Macromolecules* **1994**, *27*, 3174.
(13) Raphaël, E.; de Gennes, P. G. *J. Phys. Chem.* **1992**, *96*, 4002.
(14) Brown, H. R.; Hui, C.-Y.; Raphaël, E. *Macromolecules* **1994**, *27*, 608.
(15) Watanabe, H.; Amemiya, T.; Shimura, T.; Kotaka, T. *Macromolecules* **1994**, *27*, 2336.
(16) Yoshida, H.; Watanabe, H.; Adachi, K.; Kotaka, T. *Macromolecules* **1991**, *24*, 2981.
(17) Watanabe, H.; Shimura, T.; Kotaka, T.; Tirrell, M. *Macromolecules* **1993**, *26*, 6338.
(18) Israelachvili, J. N.; Adams, G. E. *J. Chem. Soc., Faraday Trans. 1* **1978**, *74*, 975.
(19) Horn, R. G.; Israelachvili, J. N.; Pribac, F. *J. Colloid Interface Sci.* **1987**, *115*, 480.
(20) Merrill, W. W.; Pocius, A. V.; Takker, B. V.; Tirrell, M. *Langmuir* **1991**, *7*, 1975.
(21) Johnson, K. L.; Kendall, K.; Roberts, A. D. *Proc. R. Soc. London, Ser. A* **1971**, *324*, 301.
(22) For $P > 200$ dyn the pressure at the contact spot (of $d = 0.05-0.1$ mm) is larger than 10^6 dyn/cm^2. The sugar glue exhibits plastic deformation when such a large pressure is concentrated at the small spot. (This deformation takes place more easily for the sugar glue commonly used in organic solvents than for other glues such as epoxy resins used in aqueous systems.)
(23) Israelachvili, J. N. *J. Colloid Interface Sci.* **1973**, *44*, 259.
(24) Marques, C.; Joanny, J. F.; Leibler, L. *Macromolecules* **1988**, *21*, 1051.
(25) Tsunashima, Y.; Hirata, N.; Nemoto, N.; Kurata, M. *Macromolecules* **1988**, *21*, 1007.
(26) Wu, S. Surface and Interfacial Tension of Polymers, Oligomers, Plasticizers, and Organic Pigments; In *Polymer Handbook*, 3rd ed.; Brandrup, J., Immergut, E. H., Eds.; Wiley: New York, 1989; Chapter VI.
(27) Dimarzio, E. A. *J. Chem. Phys.* **1965**, *42*, 2101.
(28) Cassasa, E. F. *J. Polym. Sci.* **1967**, *B5*, 773.
(29) Edwards, S. F.; Freed, K. F. *J. Phys. A* **1969**, *2*, 145.
(30) Doi, M.; Edwards, S. F. *The Theory of Polymer Dynamics*; Clarendon: Oxford, U.K., 1986; Chapter 2.
(31) For some cases in the experiments of Creton, Brown, and Shull,[12] the PI blocks had small σ_{PI} and should have been flattened before contact with the PI network. For those cases the PI blocks would have obtained larger conformational freedom on contact and interpenetration, and thus the conformational entropy gain would have contributed to G_0. However, in the experiments using the PI networks of *macroscopic* size, this contribution is overwhelmed by the contribution from the stretched-chain pullout mechanism.
(32) Moriguchi, S.; Udagawa, K.; Hitotsumatsu, S. *Mathematical Formulae*; Iwanami: Tokyo, 1986; Vol. II.

MA950007E